*Genij Ortopedii*. 2023;29(2):190-203.

**Original article**

https://doi.org/10.18019/1028-4427-2023-29-2-190-203

# *Models for purulent septic inflammation of the tibia in rats to assess the effect of bioresorbable materials with antimicrobial drugs*

**D.V. Smolentsev[1]✉, Yu.S. Lukina[1], L.L. Bionyshev-Abramov[1], N.B. Serezhnikova[2], M.G. Vasiliev[1], A.N. Senyagin[3], T.Ya. Pkhakadze[1]**

[1] Priorov National Medical Research Center of Traumatology and Orthopaedics, Moscow, Russian Federation

[2] Sechenov First Moscow State Medical University, Moscow, Russian Federation

[3] Peoples' Friendship University of Russia, Moscow, Russian Federation

***Corresponding author***: Dmitry V. Smolentsev, smolentsevdv@cito-priorov.ru

***Abstract***

**Introduction** A brief review of modeling purulent septic inflammation in rats, including with the help of an active bacterial agent, and methods for diagnosing inflammation are given. The **aim** of the study was to demonstrate the results of the development of an effective experimental model of purulent septic inflammation of the tibia in rats using minimally invasive methods for diagnosing infection *in vivo*. Materia**ls and methods** Various models of purulent septic inflammation were studied in four groups of small laboratory animals, when using the inoculation of *Staphylococcus aureus*. Methods for assessing purulent-septic inflammation that are not destructible by the object have been worked out: microbiological, tomographic, morphological. **Results** The results of the study indicate the possibility of creating experimental purulent-septic inflammation in rats by 14-60 days using *S. aureus* inoculation, which is a severe, rapidly progressive purulent infection that leads to extensive destruction of the bone with the formation of sequesters. **Discussion** To guarantee the formation of a purulent-inflammatory process of bone tissue in a shorter period of observation, a quantitatively controlled invasion of an active bacterial agent is necessary. A sclerosing agent and formation of a fistulous tract are not essential in creating inflammation. **Conclusion** The results of the development of experimental models for the creation of purulent-septic inflammation using minimally invasive *in vivo* diagnostic methods are demonstrated, which will allow an adequate assessment of the degree of infection before treatment.

**Keywords**: osteomyelitis, purulent-septic inflammation, bacterial invasion, golden *Staphylococcus aureu*s, sclerosing agent, inoculation, CFU

***For citation***: Smolentsev D.V., Lukina Yu.S., Bionyshev-Abramov L.L., Serezhnikova N.B., Vasiliev M.G., Senyagin A.N., Pkhakadze T.Ya. Models for purulent septic inflammation of the tibia in rats to assess the effect of bioresorbable materials with antimicrobial drugs. *Genij Ortopedii*. 2023;29(2):190-203. doi: 10.18019/1028-4427-2023-29-2-190-203

## INTRODUCTION

The problem of purulent septic infection is one of the most urgent in modern surgery. According to various authors, its incidence varies from 2 to 63.9 %, and results in osteomyelitis in 12-61 % of cases that may lead to bone necrosis and amputation with a serious risk of septicemia [1-3]. Osteomyelitis affects about 4 million people worldwide every year. In recent years, tremendous progress has been made in the treatment of infections of the musculoskeletal system; however, studies have shown that the infection rate in planned surgeries cannot be lower than 1-2 %, and failures in revision surgeries remain at the level of 33 % [4-6]. The cost of treating bone infection is substantial and will increase as the absolute number of patients suffering from it continues to rise [7].

Bone infection may develop due to direct infection (open fractures) or by spread either through the bloodstream (hematogenous) or from an adjacent site or implant [8]. Traditionally, chronic osteomyelitis has been a condition caused by the hematogenous spread of a narrow range of microorganisms, the most important of which was *Staphylococcus aureus (S. aur eus)* [1]. Recently, this category has been significantly expanded by implant-associated post-traumatic chronic osteomyelitis and contagious osteomyelitis after diabetic foot infections [9]. Moreover, 65 % of military injuries are orthopedic in nature, and the infection rate reaches 50 % [10].

The study of purulent septic processes and osteomyelitis, and namely of the pathogenesis of the disease, of diagnostic tools, effectiveness of preventive methods or various treatment options requires animal experiments. Experimental studies on animal models are often used in clinical practice, despite the difficulty of reproducing the characteristics of the infection development process in humans. The details of animal models are critical in evaluating the efficacy of antimicrobial drugs and biomaterials, especially when comparing results from different studies.

Reizner et al. conducted a large systematic review of animal models for osteomyelitis caused by *Staphylococcus aureus* [11] reported in the PubMed

and Ovid MEDLINE databases from 1902 to 2012. Of the 93 experimental studies accepted for analysis, thirty-six (38.7 %) used a rabbit as an experimental animal, most commonly the New Zealand white rabbit. Twenty-nine (31.1 %) used the rat model, most of which used Wistar or Sprague Dawley rats. Seven (7.5 %) used mice: BALB/c or C57BL/6 strains, seven (7.5 %) sheep, six (6.5 %) dogs, four (4.3 %) goats, two (2.2 %) used pigs, one (1.1 %) is guinea pigs, and one (1.1 %) is hamsters [11]. Rat models are slightly inferior to rabbit models in terms of the number of uses in experimental studies, but they are an alternative to larger animals due to their low cost and ease of maintenance. However, rats are of sufficient size to reproduce a fracture, perform drilling and fixation with screws and plates, as well as intramedullary introduction of foreign bodies, screws, pins [12].

Moreover, when selecting animals for osteomyelitis models, it must be taken into account that signs of chronic osteomyelitis, such as necrosis and severe osteolysis, develop over a shorter period of time in small animals compared to larger animals due to differences in tissue size (for example, periosteal thickness ) [2].

It is known that rats have a strong immune system, which can sometimes complicate the formation of an infection model [11]. To create acute and chronic osteomyelitis, models of an open fracture [13-15], periprosthetic osteomyelitis [16], osteomyelitis associated with external fixation [17], and a hematogenous model [18] are used.

The purpose of modeling purulent septic inflammation is to develop various protocols for therapeutic and surgical treatment. To investigate the effectiveness of new adjuvants for the treatment of osteomyelitis, it is necessary to provide an adequate solution to the clinical issues of interest. Inzana JA et al. reviewed models of bacterial creation of osteomyelitis in animals for their subsequent use in studies of polymeric, ceramic, and composite materials containing antibacterial substances [2].

Table 1 shows the results of the analysis of rat models for the study of resorbable materials.

Most studies used the rabbit model of Norden et al. [27] for osteomyelitis using a bacterial substance. *S. aureus* was inoculated into the bone marrow cavity of the proximal metaphysis of the tibia through a needle. The cortical hole was closed with bone wax, and the infection was allowed to develop within a certain period of time. A similar model has been used by other scientific groups in rats [28, 29]. Modification of the model was used in some studies with an additional placement of a Kirschner wire in the medullary canal of the tibia which was a short segment or equal to the length of the canal [25, 30-33]. Moreover, Bisland et al. initially developed a biofilm on the wire.

According to the literature, *S. aureus* is the most common causative agent of bone infections, which is a highly opportunistic species that is extremely difficult to treat [34].

In addition to the model of osteomyelitis, the result of the study is significantly influenced by the diagnostic process, which should be of high quality and uniform within the framework of one study. Along with identifying local (erythema, edema, or abscess formation) or systemic (fever or lethargy) clinical signs of infection, investigations often include advanced imaging (radiography, computed tomography (CT) or magnetic resonance imaging (MRI)), and microbiological and histological studies [11].

Some studies apply methods by which the bone and surrounding soft tissues excised [2]. However, biopsies and smears have the advantage of using a single specimen for histological analysis, thereby minimizing the number of animals needed. Histopathological tests were most frequently analyzed according to the system described by Smeltzer et al. [35]. It assigns scores from 0 to 4 to each feature based on intra-osseous acute inflammation, intra-osseous chronic inflammation, periosteal inflammation, and bone necrosis. Higher scores indicate a more severe outcome. Other scoring systems consider additional factors, including the presence of neutrophils and mononuclear cells, giant cells, fibrosis, vascularity, osteoclast activity, and abscess formation [2].

Table 1

Brief description of animal models used for studying resorbable materials [2]

| # of reference list | Bred | Region | Strain | ESR | Sclerosant/ implant | Time of infection exposure |
|---|---|---|---|---|---|---|
| [19] | Wistar | Proximal tibia | Im2-42 | Not available | none / implant | 4 weeks |
| [20] | Wistar | Proximal tibia | MSSA (ATCC 29213) | $2 \cdot 10^5$ | arachidonic acid / none | 3 weeks |
| [21, 22] | Wistar | Proximal tibia | MRSA | $2 \cdot 10^6$ | none / K-wire | 6 weeks |
| [23, 24] | Wistar | Proximal tibia | Clinical isolat MRSA | $2 \cdot 10^6$ | none / K-wire | 3 weeks |
| [25] | SD | Proximal tibia | MSSA (ATCC 49230) | $10^6$ | none / K-wire (0.2 см) | 7 weeks |
| [26] | SD | Proximal tibia | Unspecified MSSA | $10^6$ | none /none | 3 weeks |

The radiological assessment was carried out according to the system described by Norden et al. [36] and Smeltzer et al. [35]. Norden's criteria included new periosteal bone formation, sequestration, bone destruction, and extent of involvement along the tibia, where higher scores indicate worse outcome. The Smeltzer system scores periosteal elevation, architectural deformity, and new bone formation on a scale of 0 to 4, with higher scores indicating greater disease severity.

Inzana et al. state that with ongoing osteolysis, radiological imaging of improvement in successful treatment may be delayed by 4-6 weeks [2]. Other methods for visualizing the development of osteomyelitis or its treatment are microcomputed tomography (micro-CT) [37] and positron emission tomography (PET) [38].

In recent years, several research groups have begun to use bioluminescent imaging [39, 40]. With this method, bacteria are genetically modified to emit photons when they are metabolically active, after changing the lux operon.

**Our purpose** was demonstration of the results of designing experimental models for purulent septic inflammation of the rat tibia using minimally invasive methods for diagnosing infection *in vivo*.

## MATERIALS AND METHODS

The study was approved by the local ethics board at the Priorov NMRC for TO (protocol # 4 from 05 May 2021).

In all experimental models, mature males of the Wistar line weighing 250-300 g, aged from 4 to 6 months, specially bred in a certified nursery and not previously participating in the research, were used. All research procedures and conditions for keeping rodents complied with the ethical rules for working with laboratory animals, including the European Directive FELASA-2010. The animals were divided into groups using body weight as a criterion. The initial average body weight was the same in each group, and the individual weight of the animals did not differ by more than 20 % from the average weight of the animals. There were four groups: one control and three experimental. Surgical interventions were carried out in accordance with the international rules for the humane treatment of animals, under general intramuscular anesthesia with Zoletil at the rate of 7 mg/kg and Xylazine at 13 mg/kg. The modeling area was tibia of the left and right hind limbs.

A pure culture of *S. aureus* ATCC 6538 in 0.8 % agar solution based on physiological NaCl solution was used as an active bacterial agent in order to increase the viscosity of the inoculum. Inoculation of the prepared culture of *S. aureus* was carried out by catheterization through perforation holes, first into the proximal, then into the distal parts of the medullary canal, thus filling the entire canal. Systemic antibiotic therapy was administered.

The number of animals used for each model of purulent septic inflammation is presented in Table 2 and differs due to two or more repetitions of separate models over a study period of 1 year. The models used for purulent septic inflammation of the tibia of the rat are presented in Table 3.

Table 2

Number of animals used for models of purulent septic inflammation

| Model | 1 | 2 | 3 | 4 |
|---|---|---|---|---|
| Number of animals | 6 | 30 | 6 | 3 |

Microbiological study of the material from the experimental animals was carried out in accordance with generally accepted methods. In the conditions of the microbiological laboratory, the material from the animals was inoculated on solid nutrient media immediately after its delivery. Muller-Hinton agar (HIMEDIA® M211, India) with the addition of 5 % blood was used for cultivation, as well as differential diagnostic chromogenic media chromogar, uriselect, on which microorganisms of different species form colonies of different colors.

Table 3

Models of purulent septic infection

| Model No | Character and site of bone perforation | Active bacterial agent | Sclerosis agent | Sinus formation | Implants | Term of observation |
|---|---|---|---|---|---|---|
| 1 | Proximal third of the diaphysis, perforation of critical size (2/3 of bone diameter) | *S. aureus* $1.5 \cdot 10^3$ CFU in 250 mcl of nutrient medium | none | gauze turunda connecting bone perforation and the outer surface of the skin | none | 30 days |
| 2 | Diaphysis, perforation 1 mm diameter | | none | none | none | 30 days |
| 3 | Proximal tuberosity, perforation 1.2 diameter and penetration into bone canal | | none | none | pin | 60 days |
| 4 | Diaphysis, perforation with 1-mm diameter | | Burnt edges of bone perforation | none | none | 60 days |

In parallel, the material was placed in a thioglycol medium for the accumulation of microorganisms present in a limited amount, which could not be detected by direct inoculation. The cultures were treated in a thermostat at 35 ± 2°C for 24-48 hours. Bacterioscopy of prepared smears of isolated colonies evaluated tinctorial (Gram stain) and morphological properties of grown cultures.

The determination of the species of thedetected bacteria was carried out on a bacteriological analyzer "Vaitek 2 compact" (BioMerier, France). If representatives of the genus *Staphylococcus* were detected an express diagnostic "Staphylo-latex" test was used to differentiate staphylococci" (ZAO ECOlab, RF). The study was carried out on the 14th and 30th day of the experiment.

To compare the results of experiments in different groups, a scoring scale was used to assess the purity of detection:

0 points – microbes were not detected in the material;

1 point – only side flora was detected;

2 points – detection of *S. aureus* and side flora;

3 point – only *S. aureus* was detected.

Histological evaluation: the autopsy material was fixed in neutral formalin, decalcified, embedded in paraffin, cut into 4-micron thick sections, stained with hematoxylin-eosin and picrosirius red. It was studied under standard light microscopy, phase contrast and polarization microscopy in a Leica DM 4000 B LED microscope with a Leica DFC 7000 T camera.

To compare the results of the experiments in the groups, a point scale for evaluating the results was used, similar to the Smeltzer scale (Table 4).

Microcomputed tomography (micro-CT) was performed on a SkySkan 1178 scanner, at a voltage of 65 kV and a current of 615 μA, with an A1 filter of 0.5 mm. Spatial resolution was 84 μm/pixel. Sections were reconstructed using the NRecon v1.6.10.4 software; 3D reconstructions were performed using the CTVol program.

To compare the results of the experiments in the groups, a point scale for evaluating the results was used, similar to the Norden scale (Table 5).

Table 4

Point scale for evaluating results, similar to the Smeltzer scale

| Parameter | Evaluation criterion | Points |
|---|---|---|
| Acute intra-osseous inflammation | Absent | 0 |
| | From minimum to weak without abscess formation | 1 |
| | From medium to severe without abscess formation | 2 |
| | From minimum to weak with abscess formation | 3 |
| | From medium to severe with abscess formation | 4 |
| Chronic intra-osseous inflammation | Absent | 0 |
| | From minimum to weak without pronounced fibrosis | 1 |
| | From medium to severe without pronounced fibrosis | 2 |
| | From minimum to weak with pronounced fibrosis | 3 |
| | From medium to severe with pronounced fibrosis | 4 |
| Bone tissue necrosis | Absent | 0 |
| | Solitary necrotic focus without sequester | 1 |
| | Multiple foci of necrosis without sequesters | 2 |
| | Solitary sequester | 3 |
| | Multiple sequesters | 4 |

Table 5

Point scale for evaluating results, similar to the Norden scale

| Parameter | Evaluation criterion | Points |
|---|---|---|
| Sequester formation | + present | 1 |
| | - absent | 0 |
| Reactive periosteal bone formation | + present | 1 |
| | ± uncertain | 0.5 |
| | - absent | 0 |
| Bone tissue destruction | ++ extended to all bone parts | 2 |
| | + average, only in one bone part | 1 |
| | ± little, only in one bone part | 0.5 |
| | - absent | 0 |
| Changes in all bone parts (distal, diaphyseal, proximal) | + present | 1 |
| | ± uncertain | 0.5 |
| | - absent | 0 |

Statistical analysis of microbiological and tomographic examination was performed using OriginPro 2021 software. Data were recorded as mean ± standard deviation. Statistical difference between groups was determined using Tukey's test. ANOVA tests ($P < 0.05$) were used to determine the significance of differences between the groups. Significant differences $p < 0.05$ between the groups were marked with *, $p < 0.01$ between the groups – with **, $p < 0.001$ between the groups – with ***.

Statistical analysis of the experimental data of the histological examination was carried out using the GraphPad Prism 8.00 software for Windows (GraphPad Software, USA). Differences were assessed using the Kruskal-Wallis test with Dunn's multiple comparison test. P-values $\leq 0.05$ were considered statistically significant (*). The results of statistical analysis are presented as median values and interquartile range (interval between 25th and 75th percentiles).

## RESULTS

**Model 1**

No changes were observed in motor activity, hair and skin in the animals during the observation period after bacterial inoculation. In the first week after the operation, the animals spared the operated limbs; there was swelling and hyperemia of the postoperative wound edges. After 30 days, all animals showed complete healing of the postoperative wound; there were no fistulas, no purulent discharge; there was complete restoration of the integrity of the skin, except for the area of the fistulous tract formed by gauze turunda with alcohol. The edges of the fistula were epithelialized. Purulent discharge through the fistula was observed in small amounts, spontaneous fistulous tracts were not formed.

According to the data of bacteriological tests, the growth of *S. aureus* was detected in all animals after 14 days of bacterial inoculation (Table 6). Two samples showed additional contamination with intestinal flora. After 30 days of bacterial inoculation, *S. aureus* was found in 4 out of 6 samples (66.7 % of the total). At the same time, *S. aureus* monoculture was determined only in two samples.

The results of micro-CT showed a lack of regeneration (closure) of the bone perforation and pronounced tissue hyperostosis along the periphery of the bone perforation (Fig. 1). X-ray signs of a decrease in bone density along the periphery of the defect, sequestration of bone areas were noted. The axis of the limb was mostly aligned, but some deformity was noted, most likely associated with the restructuring of the bone tissue and a decrease in its strength in the zone of defect formation.

Table 6

Growth of microorganisms by days 14 and 30 in Model 1

| 14 days | 30 days | Number of animals |
|---|---|---|
| *S. aureus, E. faecalis* | *S. aureus, E. faecalis* | 2 |
| *S. aureus* | *E. coli, P. mirabilis* | 1 |
| *S. aureus* | *E. coli* | 1 |
| *S. aureus* | *S. aureus* | 2 |

The histological study revealed fragments of necrotic bone, devoid of cellular elements, found in most samples. When stained with hematoxylin and eosin, these areas showed more pronounced eosinophilia than the normal bone (Fig. 2). Phase-contrast microscopy found that the thin fibrous structure of the bone tissue was not clearly expressed; polarization microscopy found that anisotropy was sharply reduced or absent in this tissue. Degenerating bone fragments were surrounded by pronounced neutrophilic infiltration. Mosaic areas of fibrous tissue with foci of hemorrhage and inflammatory infiltration were observed in some samples. In one of the samples, bone areas with signs of regeneration were noted: more cellular elements and anisotropy by polarization microscopy was of a different nature (Fig. 3).

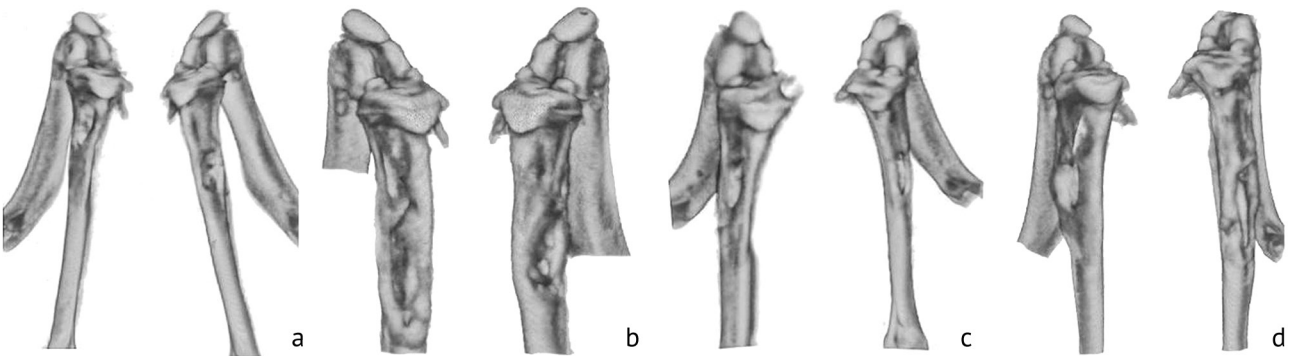


**Fig. 1** Examples of 3-D models of the animal tibia in model 1 at the time-points of the experiment: *a, c* – 0 days; *b, d* – 30 days

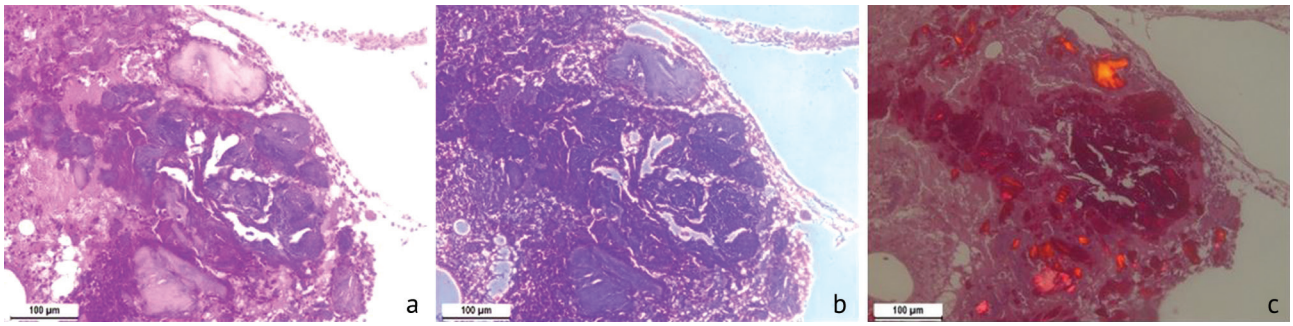


**Fig. 2** Necrotic changes in bone tissue and severe inflammation: *a* – standard light microscopy. Staining with hematoxylin-eosin; *b* – phase-contrast microscopy; *c* – polarizing microscopy. Stained with picrosirius red. Magnification 100×

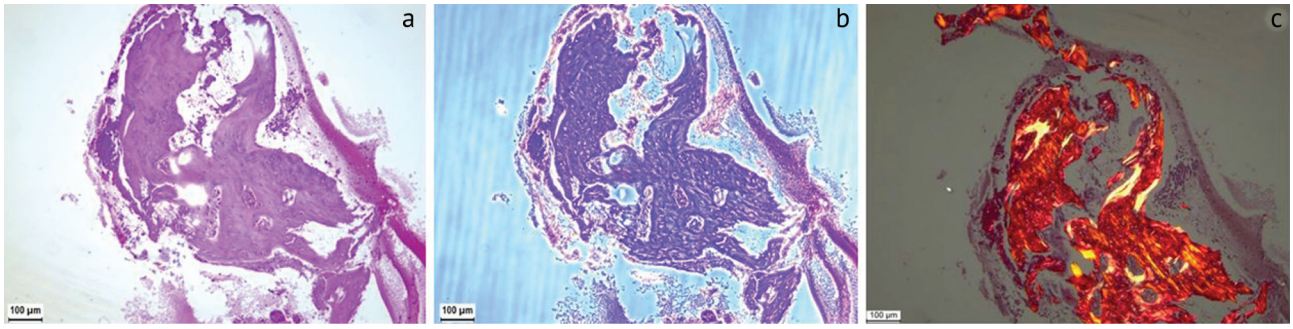


**Fig. 3**. Bone area with signs of regeneration: *a* – standard light microscopy. Staining with hematoxylin-eosin; *b* – phase-contrast microscopy; *c* – polarization microscopy. Stained with picrosirius red. Magnification 100×

**Model 2**

No changes were observed in motor activity, wool and skin in the animals during the observation period after bacterial inoculation. In the first week after the operation, the animals spared the operated limbs; swelling and hyperemia of the edges of the postoperative wound were observed. After 30 days, all animals showed complete healing of the postoperative wound, the formation of fistulas, and no purulent discharge was observed.

According to the bacteriological test, the growth of *S. aureus* was detected in all animals after 14 days of bacterial inoculation (Table 7). Two of the six samples showed additional contamination with intestinal flora. After 30 days of bacterial inoculation, *S. aureus* was found in 4 out of 6 samples (66.7 % of the total). At the same time, monoculture was determined only in two samples.

According to the results of micro-CT, there was a lack of regeneration (closure) of the bone perforation, pronounced tissue hyperostosis along the periphery of the bone perforation (Fig. 4). X-ray signs of a decrease in bone density along the periphery of the defect, sequestration of bone areas were noted; the area of the defect in some cases even increased compared to the original. The axis of the limb was deformed, which was most likely due to the restructuring of the bone tissue and a decrease in its strength in the area of defect formation.

Table 7

Growth of microorganisms by days 14 and 30 in Model 2

| 14 days | 30 days | Number of animals |
|---|---|---|
| *S. aureus* | *S. aureus* | 2 |
| *S. aureus, E. faecalis, E. coli* | *E. faecalis, E. coli* | 1 |
| *S. aureus* | *E. coli* | 1 |
| *S. aureus, P. mirabilis* | *S. aureus, P. mirabilis* | 1 |
| *S. aureus* | *S. aureus, Klebsiella* | 1 |

The histological study of biopsy specimens of that model showed that most bone fragments had dystrophic changes in the bone with a decrease in the number of osteocytes, with loosening and delamination of the bone matrix (Fig. 5a). Bone destruction also occurred with the formation of numerous small bone fragments that underwent necrosis: phase-contrast microscopy reveals a denser granular-fibrous structure in them (Fig. 5b), polarization microscopy shows no anisotropy (Fig. 5c). In the surrounding tissues, a pronounced lympho-macrophage infiltration with an admixture of neutrophils was found.

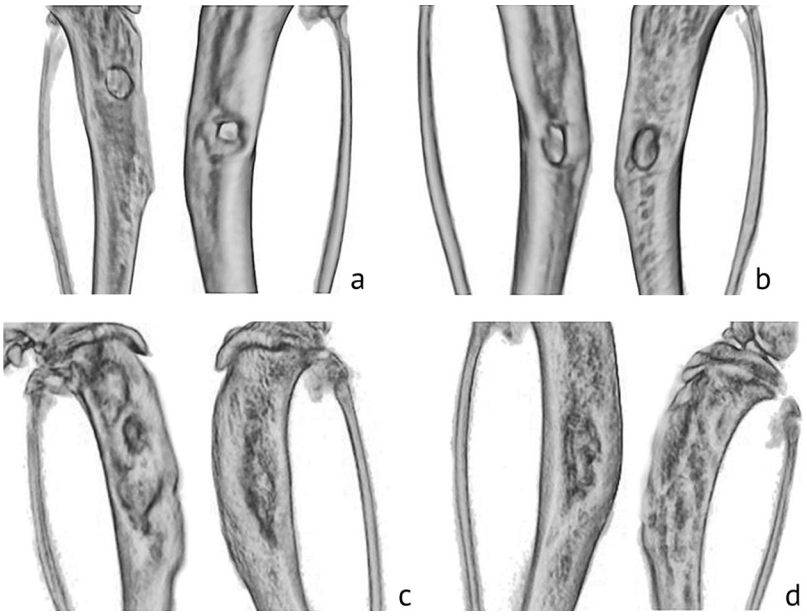


**Fig. 4** Examples of 3-D models of the animal tibia in model 2 at the time-points of the experiment: a, c – 0 days; b, d – 30 days

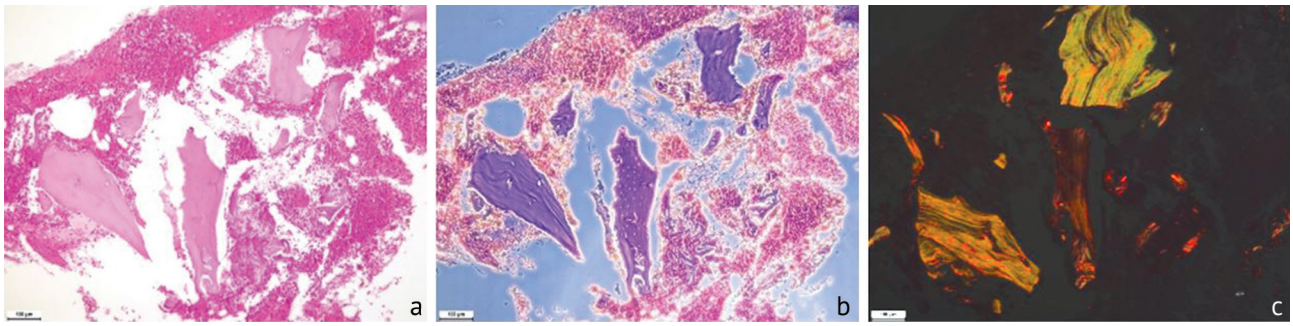


**Fig. 5** Dystrophy, destruction and necrosis of bone tissue and severe inflammation: a standard light microscopy. Staining with hematoxylin-eosin; b phase-contrast microscopy. Staining with hematoxylin-eosin; c polarization microscopy. Stained with picrosirius red. Magnification 100×

**Model 3**

No changes were observed in motor activity, wool and skin in the animals during the observation period after bacterial inoculation. In the first week after the operation, the animals spared the operated limbs; swelling and hyperemia of the edges of the postoperative wound in the zone of the pin exit were observed. After 30 days, all animals showed complete healing of the postoperative wound, spontaneous fistulous passages were not formed, but when the pin was removed, purulent discharge was noted. During the observation period, purulent discharge along the pin was not observed.

Bacteriological tests showed the growth of *S. aureus* in all animals after 14 days of bacterial inoculation (Table 8). After 30 days of bacterial inoculation, *S. aureus* was also found in all samples (100 % of the total). At the same time, *S. aureus* monoculture was determined in three samples, and mixed culture in the rest.

Model 3 was characterized by a massive infection: when the pin was removed 60 days after installation, a purulent discharge from the focus of infection was observed, which came out along with the pin.

According to the results of micro-CT, a decrease in bone density in the proximal tibia and a gap between the nail and bone tissue were observed (Fig. 6).

Migration of metal structures was not observed, however, deformities of the axis of the limb and, possibly, united fractures on the pin led to bending of the pins in some animals. It was impossible to evaluate the change in the formed defect due to overlap of the metal structure.

The results of histological study of biopsy specimens of this model were numerous necrotic bone fragments surrounded by lymphocytes, macrophages and eutrophils, sequestration was noted (Fig. 7). Biopsy specimens also contained necrotic areas in muscle and connective tissues with foci of severe inflammatory infiltration (Fig. 8).

Table 8

Growth of microorganisms by days 14 and 30 in Model 3

| 14 days | 30 days | Number of animals |
|---|---|---|
| *S. aureus* | *S. aureus* | 3 |
| *S. aureus, E. faecium* | *S. aureus, E. faecium* | 1 |
| *S. aureus* | *S. aureus, E. coli* | 1 |
| *S. aureus, P. mirabilis* | *S. aureus, P. mirabilis* | 1 |

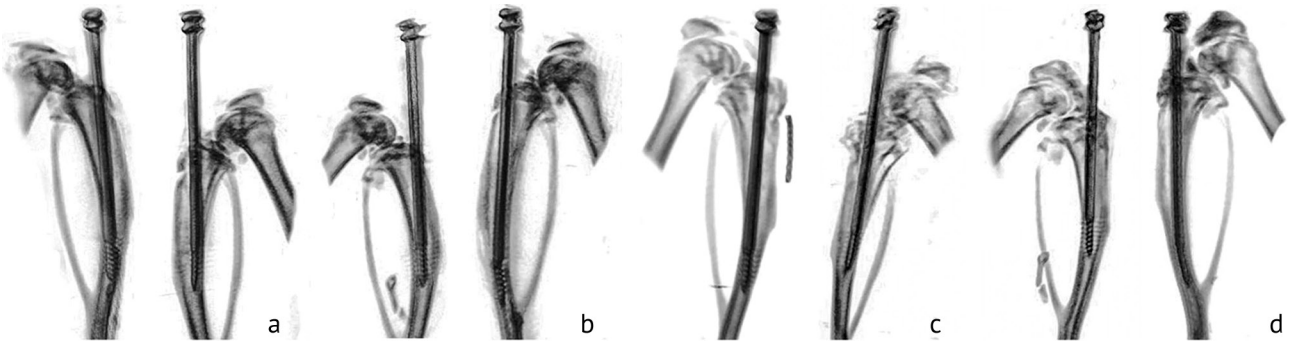


**Fig. 6** Examples of 3-D models of the animal tibia in model 3 at the time-points of the experiment: *a, c* – 0 days; *b, d* – 30 days

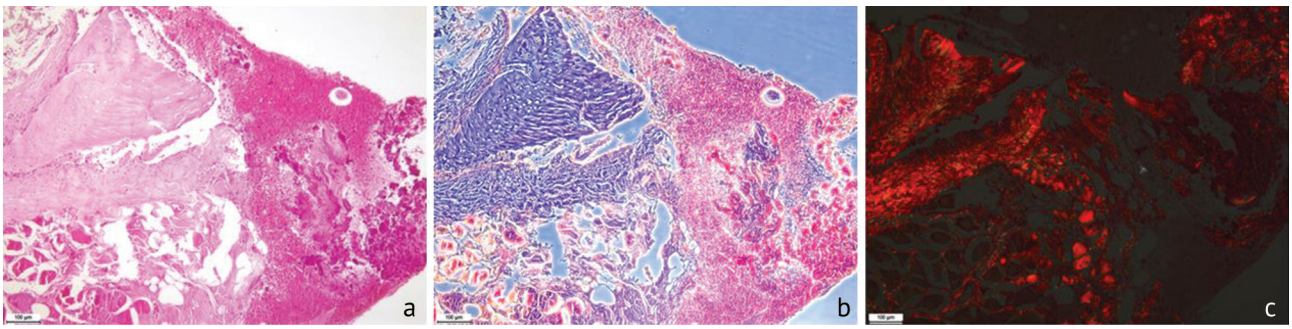


**Fig. 7** Necrosis of bone tissue, formation of sequesters and severe inflammation: *a* standard light microscopy. Staining with hematoxylin-eosin; *b* phase-contrast microscopy. Staining with hematoxylin-eosin; *c* polarization microscopy. Stained with picrosirius red. Magnification 100×

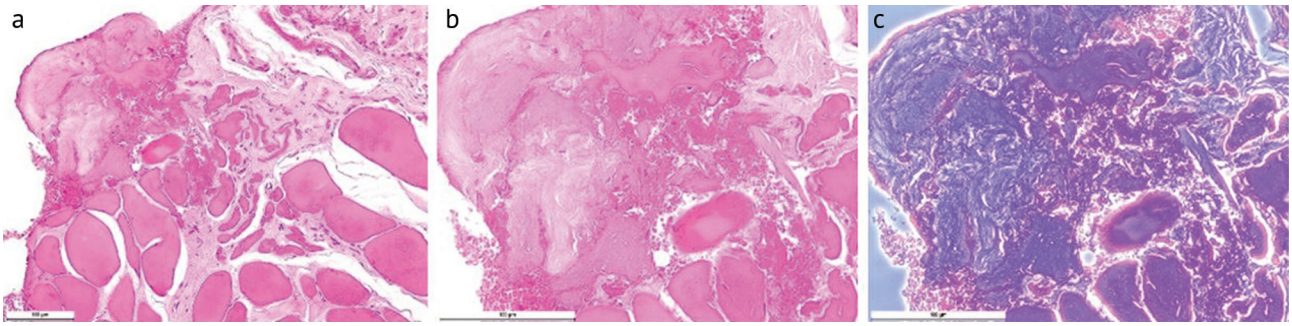


**Fig. 8** Necrotic areas in muscle and connective tissues: *a* standard light microscopy. Magnification 200×; *b* standard light microscopy. Magnification 400×; *c* phase-contrast microscopy. Magnification 400×. Hematoxylin-eosin staining

**Model 4**

No changes were observed in motor activity, wool and skin in the animals during the observation period after bacterial inoculation. In the first week after the operation, the animals spared the operated limbs; swelling and hyperemia of the edges of the postoperative wound were observed. After 30 days, all animals showed complete healing of the postoperative wound, the formation of fistulas, and no purulent discharge was observed.

Bacteriological tests revealed the growth of *S. aureus* after 14 days of bacterial inoculation in all animals (Table 7). After 30 days of bacterial inoculation, *S. aureus* was found in 5 out of 6 samples (83.3 % of the total). At the same time, *S. aureus* monoculture was determined only in one sample, and a mixed culture was determined in the rest. In addition, in one of the samples of this model, no microorganisms were detected.

The results of the microbiological study are presented in Table 9.

Table 9

Growth of microorganisms by days 14 and 30 in Model 4

| 14 days | 30 days | Number of animals |
|---|---|---|
| *S. aureus* | – | 1 |
| *S. aureus* | *S. aureus*, *S. epidermidis* | 1 |
| *S. aureus* | *S. aureus* | 1 |
| *S. aureus, E. coli* | *S. aureus, E. coli* | 1 |
| *S. aureus, E. faecium* | *S. aureus E. faecium* | 1 |
| *S. aureus, P. mirabilis* | *S. aureus, P. mirabilis* | 1 |

According to the results of micro-CT, there was an increase in the density of the contents of the bone marrow canal, the preservation of perforation or its increase, which is an indirect sign of the development of osteomyelitis. The deformity of the limb axis was less than in other groups but there were signs of bone sequestration (Fig. 9). In one animal, closure of the bone perforation was observed. One animal died on the 58th day.

The results of histological examination of biopsy specimens of this model revealed accumulation of fibrinous purulent exudate, pronounced inflammatory tissue infiltration, focal necrosis and destruction of bone tissue with loss of its fine structure (Fig. 10). In one case (deceased animal), a large abscess with necrotic detritus in the center was observed at the site of the defect, around which there was a leukocyte shaft, consisting mainly of neutrophils, and in the outer layer there was a fibrous granulation connective tissue with a pronounced inflammatory infiltration (Fig. 11).

Comparative results of a tomographic study on the models for creating purulent septic inflammation are presented in Table10 and Figure 12.

Comparative results of a microbiological study on the models for creating purulent septic inflammation are shown in Figure 13.

Comparative results of a histological study on the models of creating purulent septic inflammation are presented in Table 11.

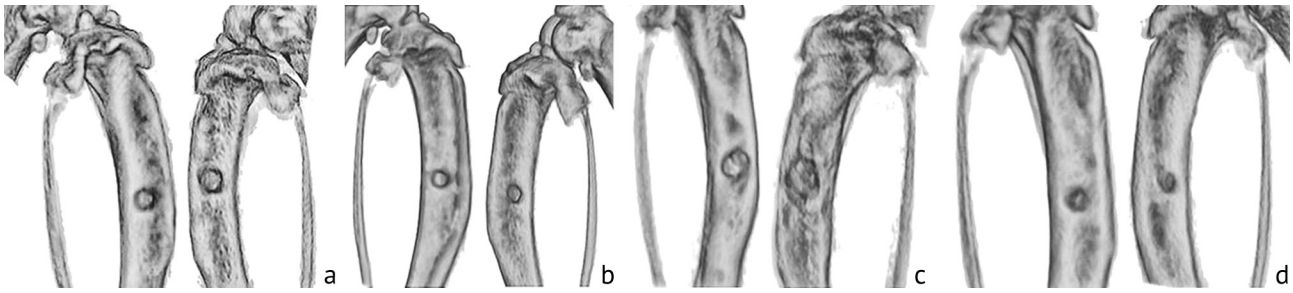


**Fig. 9** Examples of 3-D models of the animal tibia in model 4 at the time-points of the experiment: a, c – 0 days; b, d – 30 days

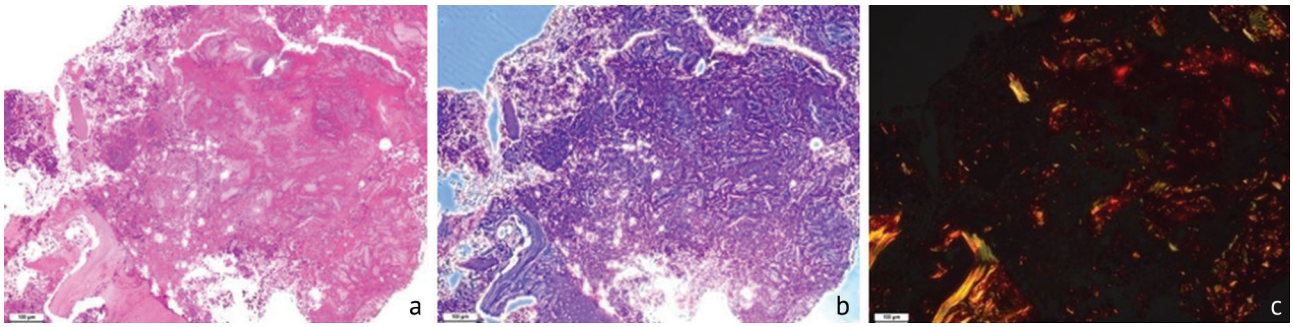


**Fig. 10** Necrotized bone fragments surrounded by inflammatory infiltrate: a standard light microscopy. Staining with hematoxylin-eosin; b phase-contrast microscopy. Staining with hematoxylin-eosin; c polarization microscopy. Staining with picrosirius red. Magnification 100×

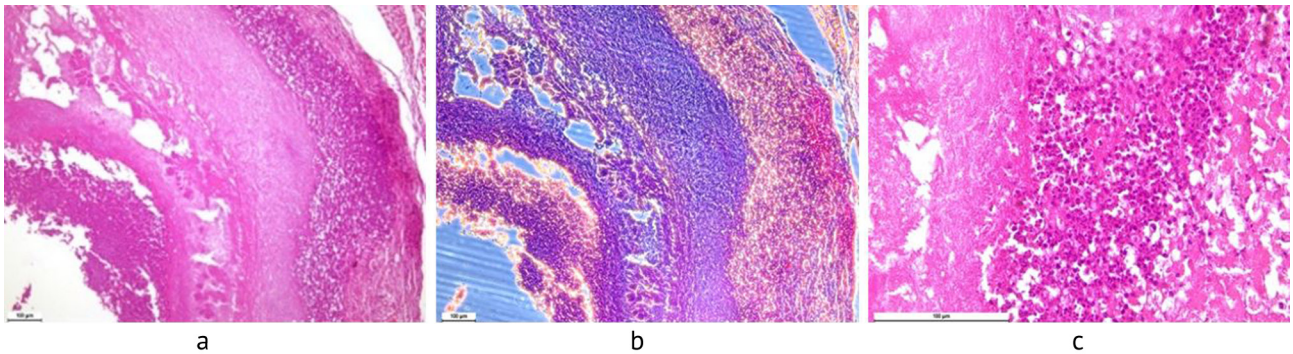


**Fig. 11** Abscess at the site of the defect: a standard light microscopy. Magnification 100×; b phase-contrast microscopy. Magnification 100×; c standard light microscopy. Magnification 400×. Hematoxylin-eosin staining

Table 10

Comparative results of tomographic study

| Model | Sequestor | Reactive periosteal bone formation | Destruction of bone tissue | Changes in bone parts |
|---|---|---|---|---|
| 1 | 0.5 ± 0.55 | 1 ± 0.0 | 0.75 ± 0.27 | 0.67 ± 0.0 |
| 2 | 0 ± 0.0 | 1 ± 0.0 | 2 ± 0.0 | 0.67 ± 0.0 |
| 3 | 1 ± 0.0 | 0.5 ± 0.0 | 2 ± 0.0 | 0.67 ± 0.0 |
| 4 | 1 ± 0.0 | 0.5 ± 0.0 | 0.33 ± 0.26 | 0.67 ± 0.0 |

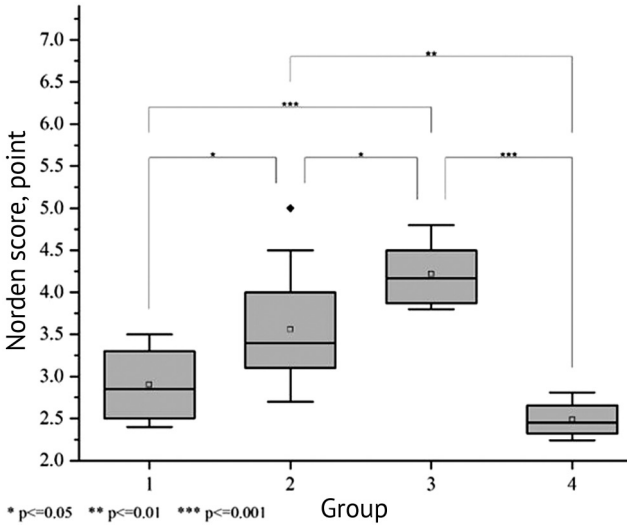


**Fig. 12** Mean values of the results of tomographic examination in the groups

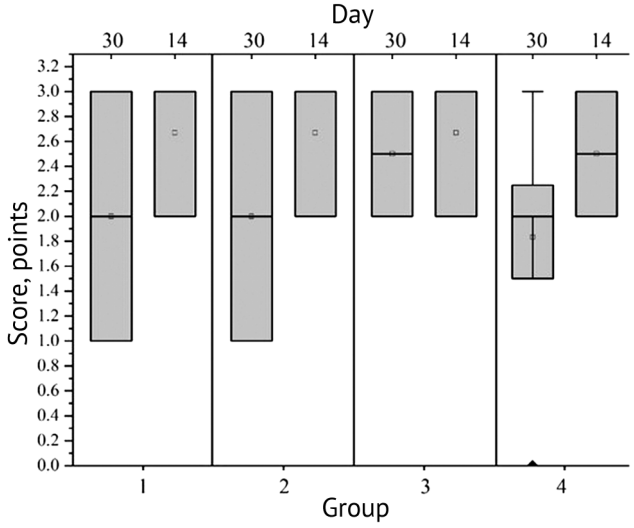


**Fig. 13** Mean values of the results of tomographic examination in the groups

Table 11

Comparative results of histological study

| Model number | Acute intra-osseous inflammation | Chronic intra-osseous inflammation | Bone necrosis | Total |
|---|---|---|---|---|
| 1 | 1 (0; 2) | 3 (2; 3) | 2 (2; 4) | 6 (4; 9) |
| 2 | 1 (1; 2) | 4 (2; 4) | 2 (2; 3) | 7 (5; 9) |
| 3 | 3 (2; 4) | 2 (1; 2) | 4 (3; 4) | 9 (6; 10) |
| 4 | 2 (2; 4) | 1 (1; 1) | 3 (2; 4) | 6 (5; 9) |
| 1 & 2 | p > 0.9999 | p > 0.9999 | p > 0.9999 | p > 0.9999 |
| 1 & 3 | p = 0.0970 | p > 0.9999 | p > 0.9999 | p > 0.9999 |
| 1 & 4 | p = 0.2997 | p = 0.1131 | p > 0.9999 | p > 0.9999 |
| 2 & 3 | p = 0.4963 | p = 0.4452 | p = 0.4907 | p > 0.9999 |
| 2 & 4 | p > 0.9999 | p = 0.0471* | p > 0.9999 | p > 0.9999 |
| 3 & 4 | p > 0.9999 | p > 0.9999 | p > 0.9999 | p > 0.9999 |

## DISCUSSION

In accordance with the literature data on the review of models for bacterial creation of osteomyelitis in animals for their subsequent use in studies of osteoplastic materials containing antibacterial substances, we conducted a comparative analysis of four models that can be used for subsequent treatment of animals using implantation of resorbable osteoplastic materials that carry antibacterial substances. The main task of the developed models and the choice of diagnostic methods is to preserve the integrity of the bone.

The results of the study show the possibility of creating experimental purulent septic inflammation in rats within 14-60 days using the inoculation of a pure culture of *S. aureus*, resulting in a severe, rapidly progressive purulent infection – osteomyelitis, leading to extensive destruction of the bone with the formation of sequesters.

The main difference in the severity of inflammation in the models used was a difference in the magnitude of bone destruction and necrosis. The positive result of creating an inflammation model is inoculation of the bacterial agent with complete filling of the medullary canal, what facilitates the spread of the bacterial agent. Some authors [41] used an allogenic bone as a carrier of an infecting

agent to localize *S. aureus* in the implantation zone. In our work, we used a 0.8 % agar solution to reduce the retrograde migration of the introduced *S. aureus* culture from the bone marrow canal back through the perforation after the catheter was removed without additional filling. The formation of an abscess in one animal in the fourth group, which we associate with the release of a bacterial agent from the bone marrow canal of the tibia, is a complication with the injection method used for administering *S. aureus*, but the number of complications is only 2 %. Thus, this method proved to be effective and does not require introduction of any materials into the bone defects thus formed, which is beneficial from the point of view of further use of the model for a subsequent study of new surgical and therapeutic protocols for the treatment of purulent septic inflammation using bioresorbable materials with antimicrobial agents.

The formation of a fistulous tract is used to localize the osteomyelitic focus in order to exclude the development of complications and death of the animal [41], usually rabbits. The creation of models of purulent septic inflammation in rats and rabbits differs significantly from each other. If, when creating a model on rabbits, the formation of a fistulous tract ensures survival, then for a model on rats, the survival rate of animals is 98 % in all presented models, which is associated with a strong immune system. In this regard, we can conclude that the formation of a fistulous tract is not a necessity for creating purulent septic inflammation in rats.

When *S. aureus* was inoculated through a bone perforation hole, regardless of its size, a change in the anatomical shape of the tibia was observed in all models. Low doses of the active bacterial agent ($1.5 \times 10^3$ CFU) are less effective in creating purulent septic inflammation, although, according to the literature, the optimal inoculation doses of the culture for rats varied in the range of 103-106 CFU, and some models of open fractures use only 102 CFU [11]. It is likely that such low doses can be effective when using intraosseous systems in conjunction with inoculation. At a concentration of *S. aureus* of 1.5×103 CFU, the physiological shape of the bone changes in less than half of the cases; hyperostosis was observed only along the edges of bone perforation, and the manifestation of signs characteristic of osteomyelitis varied. An increase in the concentration of *S. aureus* by 1000 times leads to the development of persistent infections in most cases.

The changes observed on CT scan correlated with nearly identical histological findings. Characteristic signs of osteomyelitis – dystrophy, destruction, necrosis of bone tissue, inflammatory infiltration of surrounding tissues – were observed to a greater extent with inoculation of *S. aureus* $1.5 \times 10^6$ CFU. Purulent destructive necrosis is characteristic of infection caused by staphylococci [36]. The highest rates of bone tissue necrosis, according to the histological tests were observed when using models 3 and 4, which, in our opinion, is associated with a longer period after staphylococcus inoculation. The indicator of chronic intra-osseous inflammation was the highest in the second group, and the differences in this parameter between the fourth and second groups are statistically significant.

Swab cultures obtained from inoculation sites confirmed the presence of *S. aureus* after 14 days in all samples. After 30 days, *S. aureus* was not detected in the swabs of 21 % of the samples. Gram-positive enterococci *E. faecium* and gram-negative bacteria *E. coli* and *P. mirabilis*, belonging to the intestinal flora, were found instead of *S. aureus*, which may indicate contamination of the wound canal in the postoperative period.

A sclerosing agent can be used;however, according to our observations, it has little effect on the formation of purulent septic inflammation. With the high efficiency of infection of model 4 animals, one recovery was observed in six cases. According to the literature, 5 % sodium morriat and arachidonic acid have been used as sclerosing agents in modeling osteomyelitis in animals. Buxton et al., when modeling an open fracture, interrupted the endosteal blood supply by cauterization, after which bacterial contamination was performed [15]. On the one hand, local disturbance of microcirculation and focal necrosis make the bone more susceptible to infection, on the other hand, they can artificially distort the results of treatment studies, especially those based on the distribution of systemic antibiotics along the vessels 2].

Foreign body implantation increases susceptibility to infections and is an alternative to sclerosing agents. When a pin is inserted into the medullary canal, a persistent purulent infection is observed, which is probably associated with the formation of a biofilm on the surface of the implant and inside the bone [42]. Bacteria inside the biofilm can evade the host's immunological response and often enter a dormant or dormant state [43], which can reduce the effectiveness of antibiotics and require a significant increase in the minimum effective concentration of the drug [44]. Moreover, additional intervention is required to remove the pin before therapeutic or surgical treatment. These points must be considered while choosing a model.

Thus, we consider the method of model 2 to be the most technically simple and effective for creating purulent septic inflammation. The applicability of the developed models for use as experimental ones in biomedical studies of osteoplastic materials with antibacterial properties requires a separate research, but the main requirement for the model, to preserve the integrity of the bone, has been met.

In the scientific literature, to confirm the effectiveness of creating purulent-septic inflammation by various

methods, as a rule, animals are withdrawn from the experiment [41, 45]. In the works on the study of the effectiveness of the developed materials for the treatment of purulent septic inflammation, complex diagnostic methods are used after the withdrawal of animals from the experiment [20-24]. X-rays and assessment of clinical signs were used by some authors [25], microbiological and radiological assessments by others [26]. The complete absence or partial diagnosis does not allow assessment the severity of inflammation before treatment, the interpretation of the results of treatment may be false. In our work, we used tomographic, microbiological and histological methods to detect infection. With many existing methods for analyzing a bacterial infection, our task was to assess the presence and severity of purulent septic inflammation using minimally invasive *in vivo* diagnostic methods to obtain initial data before therapeutic or surgical treatment. This is necessary for subsequent evaluation of the effectiveness of treatment and interpretation of its results.

According to our observations, the degree of infection can most reliably be determined using a combination of tomographic, histological and microbiological studies. Thus, bacterial infection within the bone can be highly variable and spatially heterogeneous, and swabs probably may give false negative results. Tomographic assessment allows visualization of bone infection by periosteal reaction, osteolysis, soft tissue edema, deformity, sequestration, spontaneous fracture, but improvements may lag behind treatment. If intraosseous implants are used, the effectiveness of tomographic evaluation is significantly reduced due to artifacts from metal parts. Histological assessment of biopsy specimens evaluates the presence of morphological features characteristic of osteomyelitis: bone tissue necrosis and inflammatory infiltration. But a histological study alone cannot verify the degree of manifestation of these signs as they can vary significantly depending on the site of collection, the size and number of biopsy specimens, therefore, an integrated approach yields a more objective and representative picture of the course of the osteomyelitis process.

The combined use of these minimally invasive *in vivo* diagnostic methods enables to obtain an adequate assessment of the degree of infection before treatment.

## CONCLUSION

The results of the development of four experimental models for the creation of purulent septic inflammation of the tibia in rats have been demonstrated. In all models, bacterial culture of *Staphylococcus aureus* was inoculated at a concentration of $1.5 \times 10^3$ or $1.5 \times 10^6$ CFU in an agar solution into the bone marrow canal of the tibia in rats. The models differ in the concentration of the bacterial agent, the use of a sclerosing agent, the formation of a fistulous tract, or the use of an intramedullary nail.

All the described models are suitable for creating purulent septic inflammation, however, the most technically simple method is filling the bone marrow canal with a bacterial agent by inoculating the latter in an agar solution without using a sclerosing agent, implanting foreign bodies, or forming a fistulous tract. The proposed method is well reproducible and allows development of purulent septic inflammation within 30 days.

The work shows that the known methods of diagnosis (tomographic, microbiological and histological studies) together are an effective method for determining the level of infection without destroying the object. This is important for obtaining initial data before therapeutic or surgical treatment, what enables to subsequently evaluate the effectiveness of treatment and interpret its results.

Thus, we managed to achieve our goal by demonstrating the results of developing experimental models of purulent septic inflammation using minimally invasive *in vivo* diagnostic methods, which will allow us to obtain an adequate assessment of the degree of infection before treatment.

## REFERENCES


1. Lew DP, Waldvogel FA. Osteomyelitis. *Lancet*. 2004;364(9431):369-79. doi: 10.1016/S0140-6736(04)16727-5
2. Inzana JA, Schwarz EM, Kates SL, Awad HA. Biomaterials approaches to treating implant-associated osteomyelitis. *Biomaterials*. 2016;81:58-71. doi: 10.1016/j.biomaterials.2015.12.012
3. Rao N, Lipsky BA. Optimising antimicrobial therapy in diabetic foot infections. *Drugs*. 2007;67(2):195-214. doi: 10.2165/00003495-200767020-00003
4. Cram P, Lu X, Kates SL, Singh JA, Li Y, Wolf BR. Total knee arthroplasty volume, utilization, and outcomes among Medicare beneficiaries, 1991-2010. *JAMA*. 2012;308(12):1227-36. doi: 10.1001/2012.jama
5. Rosas S, Ong AC, Buller LT, Sabeh KG, Law TY, Roche MW, Hernandez VH. Season of the year influences infection rates following total hip arthroplasty. *World J Orthop*. 2017;8(12):895-901. doi: 10.5312/wjo.v8.i12.895
6. Geurts JAP, van Vugt TAG, Arts JJC. Use of contemporary biomaterials in chronic osteomyelitis treatment: Clinical lessons learned and literature review. *J Orthop Res*. 2021;39(2):258-264. doi: 10.1002/jor.24896
7. Schwarz EM, Parvizi J, Gehrke T, Aiyer A, Battenberg A, Brown SA, Callaghan JJ, Citak M, Egol K, Garrigues GE, Ghert M, Goswami K, Green A, Hammound S, Kates SL, McLaren AC, Mont MA, Namdari S, Obremskey WT, O'Toole R, Raikin S, Restrepo C, Ricciardi B, Saeed K, Sanchez-Sotelo J, Shohat N, Tan T, Thirukumaran CP, Winters B. 2018 International Consensus Meeting on Musculoskeletal Infection: Research Priorities from the General Assembly Questions. *J Orthop Res*. 2019;37(5):997-1006. doi: 10.1002/jor.24293
8. Sheehy SH, Atkins BA, Bejon P, Byren I, Wyllie D, Athanasou NA, Berendt AR, McNally MA. The microbiology of chronic osteomyelitis: prevalence of resistance to common empirical anti-microbial regimens. J Infect. 2010;60(5):338-43. doi: 10.1016/j.jinf.2010.03.006

9. Trampuz A, Zimmerli W. Diagnosis and treatment of infections associated with fracture-fixation devices. *Injury*. 2006;37 Suppl 2:S59-66. doi: 10.1016/j.injury.2006.04.010
10. Murray CK, Hsu JR, Solomkin JS, Keeling JJ, Andersen RC, Ficke JR, Calhoun JH. Prevention and management of infections associated with combat-related extremity injuries. *J Trauma*. 2008;64(3 Suppl):S239-51. doi: 10.1097/TA.0b013e318163cd14
11. Reizner W, Hunter JG, O'Malley NT, Southgate RD, Schwarz EM, Kates SL. A systematic review of animal models for Staphylococcus aureus osteomyelitis. *Eur Cell Mater*. 2014 25;27:196-212. doi: 10.22203/ecm.v027a15
12. Histing T, Garcia P, Holstein JH, Klein M, Matthys R, Nuetzi R, Steck R, Laschke MW, Wehner T, Bindl R, Recknagel S, Stuermer EK, Vollmar B, Wildemann B, Lienau J, Willie B, Peters A, Ignatius A, Pohlemann T, Claes L, Menger MD. Small animal bone healing models: standards, tips, and pitfalls results of a consensus meeting. *Bone*. 2011;49(4):591-9. doi: 10.1016/j.bone.2011.07.007
13. Lindsey BA, Clovis NB, Smith ES, Salihu S, Hubbard DF. An animal model for open femur fracture and osteomyelitis: Part I. *J Orthop Res*. 2010;28(1):38-42. doi: 10.1002/jor.20960
14. Li B, Jiang B, Dietz MJ, Smith ES, Clovis NB, Rao KM. Evaluation of local MCP-1 and IL-12 nanocoatings for infection prevention in open fractures. *J Orthop Res*. 2010;28(1):48-54. doi: 10.1002/jor.20939
15. Buxton TB, Travis MT, O'Shea KJ, McPherson JC 3rd, Harvey SB, Plowman KM, Walsh DS. Low-dose infectivity of Staphylococcus aureus (SMH strain) in traumatized rat tibiae provides a model for studying early events in contaminated bone injuries. *Comp Med*. 2005;55(2):123-128.
16. Antoci V Jr, Adams CS, Hickok NJ, Shapiro IM, Parvizi J. Vancomycin bound to Ti rods reduces periprosthetic infection: preliminary study. *Clin Orthop Relat Res*. 2007;461:88-95. doi: 10.1097/BLO.0b013e318073c2b2
17. Holt J, Hertzberg B, Weinhold P, Storm W, Schoenfisch M, Dahners L. Decreasing bacterial colonization of external fixation pins through nitric oxide release coatings. *J Orthop Trauma*. 2011;25(7):432-437. doi: 10.1097/BOT.0b013e3181f9ac8a
18. Hienz SA, Sakamoto H, Flock JI, Mörner AC, Reinholt FP, Heimdahl A, Nord CE. Development and characterization of a new model of hematogenous osteomyelitis in the rat. *J Infect Dis*. 1995;171(5):1230-1236. doi: 10.1093/infdis/171.5.1230
19. Itokazu M, Yamamoto K, Yang WY, Aoki T, Kato N, Watanabe K. The sustained release of antibiotic from freeze-dried fibrin-antibiotic compound and efficacies in a rat model of osteomyelitis. *Infection*. 1997;25(6):359-363. doi: 10.1007/BF01740818
20. Mendel V, Simanowski HJ, Scholz HC, Heymann H. Therapy with gentamicin-PMMA beads, gentamicin-collagen sponge, and cefazolin for experimental osteomyelitis due to Staphylococcus aureus in rats. *Arch Orthop Trauma Surg*. 2005;125(6):363-368. doi: 10.1007/s00402-004-0774-2
21. Cevher E, Orhan Z, Mülazimoğlu L, Sensoy D, Alper M, Yildiz A, Ozsoy Y. Characterization of biodegradable chitosan microspheres containing vancomycin and treatment of experimental osteomyelitis caused by methicillin-resistant Staphylococcus aureus with prepared microspheres. *Int J Pharm*. 2006;317(2):127-135. doi: 10.1016/j.ijpharm.2006.03.014
22. Orhan Z, Cevher E, Mülazimoglu L, Gürcan D, Alper M, Araman A, Ozsoy Y. The preparation of ciprofloxacin hydrochloride-loaded chitosan and pectin microspheres: their evaluation in an animal osteomyelitis model. *J Bone Joint Surg Br*. 2006;88(2):270-275. doi: 10.1302/0301-620X.88B2.16328
23. Cevher E, Orhan Z, Sensoy D, Ahiskali R, Kan PL, Sağirli O, Mülazimoğlu L. Sodium fusidate-poly(D,L-lactide-co-glycolide) microspheres: preparation, characterisation and in vivo evaluation of their effectiveness in the treatment of chronic osteomyelitis. *J Microencapsul*. 2007;24(6):577-595. doi: 10.1080/02652040701472584
24. Orhan Z, Cevher E, Yildiz A, Ahiskali R, Sensoy D, Mülazimoğlu L. Biodegradable microspherical implants containing teicoplanin for the treatment of methicillin-resistant Staphylococcus aureus osteomyelitis. *Arch Orthop Trauma Surg*. 2010;130(1):135-142. doi: 10.1007/s00402-009-0886-9
25. Solberg BD, Gutow AP, Baumgaertner MR. Efficacy of gentamycin-impregnated resorbable hydroxyapatite cement in treating osteomyelitis in a rat model. *J Orthop Trauma*. 1999;13(2):102-106. doi: 10.1097/00005131-199902000-00006
26. Zelken J, Wanich T, Gardner M, Griffith M, Bostrom M. PMMA is superior to hydroxyapatite for colony reduction in induced osteomyelitis. *Clin Orthop Relat Res*. 2007;462:190-194. doi: 10.1097/BLO.0b013e3180ca9521
27. Norden CW. Experimental osteomyelitis. I. A description of the model. *J Infect Dis*. 1970;122(5):410-418. doi: 10.1093/infdis/122.5.410
28. Subasi M, Kapukaya A, Kesemenli C, Kaya H, Sari I. Effect of granulocyte-macrophage colony-stimulating factor on treatment of acute osteomyelitis. An experimental investigation in rats. *Arch Orthop Trauma Surg*. 2001;121(3):170-173. doi: 10.1007/s004020000209
29. Burch S, Bisland SK, Bogaards A, Yee AJ, Whyne CM, Finkelstein JA, Wilson BC. Photodynamic therapy for the treatment of vertebral metastases in a rat model of human breast carcinoma. *J Orthop Res*. 2005;23(5):995-1003. doi: 10.1016/j.orthres.2004.12.014
30. Ersoz G, Oztuna V, Coskun B, Eskandari MM, Bayarslan C, Kaya A. Addition of fusidic acid impregnated bone cement to systemic teicoplanin therapy in the treatment of rat osteomyelitis. *J Chemother*. 2004;16(1):51-55. doi: 10.1179/joc.2004.16.1.51
31. Lucke M, Schmidmaier G, Sadoni S, Wildemann B, Schiller R, Stemberger A, Haas NP, Raschke M. A new model of implant-related osteomyelitis in rats. *J Biomed Mater Res B Appl Biomater*. 2003;67(1):593-602. doi: 10.1002/jbm.b.10051
32. Bisland SK, Chien C, Wilson BC, Burch S. Pre-clinical in vitro and in vivo studies to examine the potential use of photodynamic therapy in the treatment of osteomyelitis. *Photochem Photobiol Sci*. 2006;5(1):31-38. doi: 10.1039/b507082a
33. García-Alvarez F, Navarro-Zorraquino M, Castro A, Grasa JM, Pastor C, Monzón M, Martínez A, García-Alvarez I, Castillo J, Lozano R. Effect of age on cytokine response in an experimental model of osteomyelitis. *Biogerontology*. 2009;10(5):649-658. doi: 10.1007/s10522-008-9211-1
34. Darouiche RO. Treatment of infections associated with surgical implants. *N Engl J Med*. 2004;350(14):1422-1429. doi: 10.1056/NEJMra035415
35. Smeltzer MS, Thomas JR, Hickmon SG, Skinner RA, Nelson CL, Griffith D, Parr TR Jr, Evans RP. Characterization of a rabbit model of staphylococcal osteomyelitis. *J Orthop Res*. 1997;15(3):414-421. doi: 10.1002/jor.1100150314
36. Norden CW, Myerowitz RL, Keleti E. Experimental osteomyelitis due to Staphylococcus aureus or Pseudomonas aeruginosa: a radiographic-pathological correlative analysis. *Br J Exp Pathol*. 1980;61(4):451-460.
37. Inzana JA, Trombetta RP, Schwarz EM, Kates SL, Awad HA. 3D printed bioceramics for dual antibiotic delivery to treat implant-associated bone infection. *Eur Cell Mater*. 2015;30:232-247. doi: 10.22203/ecm.v030a16
38. Koort JK, Mäkinen TJ, Suokas E, Veiranto M, Jalava J, Knuuti J, Törmälä P, Aro HT. Efficacy of ciprofloxacin-releasing bioabsorbable osteoconductive bone defect filler for treatment of experimental osteomyelitis due to Staphylococcus aureus. *Antimicrob Agents Chemother*. 2005;49(4):1502-1508. doi: 10.1128/AAC.49.4.1502-1508.2005
39. Li D, Gromov K, Søballe K, Puzas JE, O'Keefe RJ, Awad H, Drissi H, Schwarz EM. Quantitative mouse model of implant-associated osteomyelitis and the kinetics of microbial growth, osteolysis, and humoral immunity. *J Orthop Res*. 2008;26(1):96-105. doi: 10.1002/jor.20452
40. Kadurugamuwa JL, Sin L, Albert E, Yu J, Francis K, DeBoer M, Rubin M, Bellinger-Kawahara C, Parr TR Jr, Contag PR. Direct continuous method for monitoring biofilm infection in a mouse model. *Infect Immun*. 2003;71(2):882-890. doi: 10.1128/IAI.71.2.882-890.2003
41. Korolev SB, Mitrofanov VN, Zhivtsov OP, Orlinskaya NYu, Yulina DP. Simulation of experimental chronic osteomyelitis. *Genij Ortopedii*. 2022;28(2):223-227. doi: 10.18019/1028-4427-2022-28-2-223-227
42. Waeiss RA, Negrini TC, Arthur RA, Bottino MC. Antimicrobial effects of drug-containing electrospun matrices on osteomyelitis-associated pathogens. *J Oral Maxillofac Surg*. 2014;72(7):1310-1319. doi: 10.1016/j.joms.2014.01.007
43. Rani SA, Pitts B, Beyenal H, Veluchamy RA, Lewandowski Z, Davison WM, Buckingham-Meyer K, Stewart PS. Spatial patterns of DNA replication, protein synthesis, and oxygen concentration within bacterial biofilms reveal diverse physiological states. *J Bacteriol*. 2007;189(11):4223-4233. doi: 10.1128/JB.00107-07

44. Mihailescu R, Furustrand Tafin U, Corvec S, Oliva A, Betrisey B, Borens O, Trampuz A. High activity of Fosfomycin and Rifampin against methicillin-resistant staphylococcus aureus biofilm in vitro and in an experimental foreign-body infection model. *Antimicrob Agents Chemother*. 2014;58(5):2547-2553. doi: 10.1128/AAC.02420-12
45. O'Reilly T, Mader JT. Rat model of bacterial osteomyelitis of the tibia. In: Zak O, Sande MA, editors. Handbook of Animal Models of Infection: Experimental Models in Antimicrobial Chemotherapy. San Diego, CA: Academic Press. (1999), p. 561-575. doi: 10.1016/B978-012775390-4/50205-0

The article was submitted 24.11.2022; approved after reviewing 16.01.2023; accepted for publication 20.02.2023.

**Information about the authors:**

1. Dmitry V. Smolentsev – smolentsevdv@cito-priorov.ru, https://orcid.org/0000-0001-5386-1929;
2. Yulia S. Lukina – Candidate of Technical Sciences, lukina_rctu@mail.ru, https://orcid.org/0000-0003-0121-1232;
3. Leonid L. Bionyshev-Abramov – sity-x@bk.ru, https://orcid.org/0000-0002-1326-6794;
4. Natalya B. Serezhnikova – Candidate of Biological Sciences, natalia.serj@yandex.ru, https://orcid.org/0000-0002-4097-1552;
5. Maxim G. Vasiliev – Candidate of Medical Sciences, maxox@mail.ru, https://orcid.org/0000-0001-9810-6513;
6. Aleksandr N. Senyagin – senyagin_an@pruf.ru, https://orcid.org/0000-0002-4981-0149;
7. Tamara Ya. Pkhakadze – Doctor of Medical Sciences, microlab_cito@mail.ru, https://orcid.org/0000-0003-4900-3555.

**Contribution of the authors:**

Lukina Yu.S., Smolentsev D.V. – idea; formulation of the goals and objectives of the study; methodology development; creating models; checking the reproducibility of the study results; statistical analysis of study data; conducting research; data collection and processing; preparation and writing of the initial version of the work; editing and preparing work for publication; control and management of research work; responsibility for managing and coordinating the planning and conduct of research performance.
Bionyshev-Abramov L.L. – development of methodology; creating models; checking the reproducibility of the study results; statistical analysis of study data; conducting research; data collection and processing; preparation and writing of the initial version of the work; preparing work for publication.
Vasiliev M.G., Serezhnikova N.B., Pkhakadze T.Ya. – research performance; data collection.
Senyagin A.N. – data processing.

***Conflict of interests*** *Not applicable.*

***Funding*** *The study was carried out within the framework of the state assignment to the Federal State Budgetary Institution Priorov NMRC for TO of the Ministry of Health of Russia "Development of a technology for obtaining osteoplastic polymeric and calcium-phosphate materials with a controlled release rate of antibiotics and target pharmaceutical substances for the surgical treatment of purulent processes in bone tissue and the prevention of the formation of bacterial biofilms on implantable metal structures."*

***Ethics approval*** *The study was approved at the ethics board meeting, ptotocol 4 dated 05 May 2021.*

***Informed consent*** *Not applicable.*